PRAMANA
— journal of
physics

Vol. 67, No. 6
December 2006
pp. 1087–1097

Measurement of storage time, estimation of ion number and study of absorption line profile in a Paul trap

SOUMEN BHATTACHARYYA, ANITA GUPTA, S G NAKHATE and PUSHPA M RAO*
Spectroscopy Division, Bhabha Atomic Research Centre, Mumbai 400 085, India
*Corresponding author. E-mail: pushpam@magnum.barc.ernet.in

MS received 12 June 2006; revised 11 August 2006; accepted 22 August 2006

Abstract. Europium (Eu^+) ions were confined in a Paul trap and detected by non-destructive method. Storage time of Eu^+ ions achieved in vacuum was improved by orders of magnitude employing buffer gas cooling. The experimentally detected signal was fitted to the ion response signal and the total number of ions trapped was estimated. It is found that the peak signal amplitude as well as the product of FWHM and the peak signal amplitude is proportional to the total number of trapped ions. The trapped ion secular frequency was swept at different rates and its effect on the absorption line profile was studied both experimentally and theoretically.

Keywords. Quadrupole ion trap; storage time; line profile analysis.

PACS Nos 32.80.Pj; 33.80.Ps; 39.10.+j; 42.50.Vk

1. Introduction

Ever since its advent, Paul traps have been used for a wide range of applications such as mass spectrometry [1], precision measurements of hyperfine structures [2], frequency standards both in the microwave and optical regions [3], lifetime measurements of metastable states and atomic collision studies [4] to name a few. Confinement of ions offers unique advantages: (a) the trapped particles are free from any external uncontrollable perturbations, (b) long storage times enable prolonged probing of the ions, (c) efficient usage of rare isotopes under study, (d) ion trap offers a well-characterized environment which allows the study of oscillation frequencies of confined ions. High-resolution mass spectrometry in particular demands narrow well-defined resonance lines for which the characterization and the study of the dynamics of the trapped ion cloud are of paramount importance.

Several methods are employed for the detection of trapped ions [5] depending on the particles trapped and type of studies to be performed. In the non-destructive

detection technique, the ions remain in the trap after detection and both electronic as well as optical methods can be employed. The electronic detection technique measures the response of the mass-dependent oscillation frequencies of ions in the trap, to the external probing dipole field, by a tank circuit coupled to the ion trap [6]. The sensitivity of this method depends on the quality factor Q of the resonance circuit and the technique allows detection of any trapped particle. Though optical detection is the most sensitive method allowing detection of even a single ion [7], it is restricted to ions, which have energy level schemes that allow excitation by available lasers. However, for the determination of the total number of trapped ions, the ion oscillation amplitudes should be of the order of the laser beam diameter. The destructive detection technique employing the ejection and collection of trapped ions onto a particle detector is a quite sensitive method but requires a constant supply of ions.

In our work non-destructive electronic detection technique is employed. Prior to conducting any laser spectroscopic investigations, estimation of the storage time and the total number of ions trapped is important. In the present work, europium ions (Eu^+) are taken up as we plan to carry out spectroscopic investigations on this ion in future. However, our results apply to any trapped ions.

The storage time of the trapped ion is defined as the time during which the ion number decreases to $1/e$ of the original number [8]. Cooling the hot ions dramatically improves the storage time. There are several methods of cooling and one of the simplest method is the viscous damping of the ion oscillations using a light buffer gas [9], which is employed in the present work. We describe the line profile analysis of the detected signal for the estimation of the trapped ion number [10].

Goeringer *et al* [11] have employed resonance ejection detection method and predict an increase in mass resolution with decreasing sweep rate in the Paul trap mass spectrometer. The destructive resonance ejection detection method, suffers from the distortion of the trapping potential due to the applied ejection pulse, leading to non-linear effects [12]. In this context the study of dynamic response of the trapped ions to a weak probing field, minimizing the distortion of the applied trapping is important. We have simulated the absorption line profile at different sweep rates and compared it with the experimental data.

Quadrupole ion trap typically comprises of a three-electrode structure, one ring and two end caps, whose inner surfaces are hyperboloids. An RF potential in conjunction with a DC potential is applied between the ring electrode and the end caps. The resulting potential is given as

$$\phi(r, z) = \frac{\phi_0}{2r_0^2}[x^2 + y^2 - 2z^2], \tag{1}$$

where potential ϕ_0 is of the form $U_{\mathrm{DC}} + V_{\mathrm{AC}} \cos(\Omega t)$ and r_0 is the trap radius.

The equations of motion for the ion trajectories is in the form of Mathieu equations

$$\frac{\mathrm{d}^2 x_i}{\mathrm{d}\tau^2} + (a_i - 2q_i \cos 2\tau)x_i = 0; \quad i = r, z \tag{2}$$

and the scaled time $\tau = \frac{1}{2}\Omega t$.

The stability domain of the ion trajectories are governed by the solutions of Mathieu equations [13,14] and basically depend on the trapping parameters $-a_z = 2a_r = 8eU_{\rm DC}/m\Omega^2 r_0^2$ and $q_z = -2q_r = 4eV_{\rm AC}/m\Omega^2 r_0^2$, where m is the mass and e is the charge of the trapped ion, Ω is the frequency of the trapping field.

In the pseudopotential approximation [15] the ion motion is depicted as composed of a small amplitude but high-frequency micromotion δ superimposed on a slowly varying but larger amplitude secular motion Z. Thus with $z = Z + \delta$, the axial motion of the ions is described by

$$\frac{{\rm d}^2 Z}{{\rm d}t^2} + \omega_z^2 Z = 0 \tag{3}$$

and here t is the natural time.

In an ideal trap and particularly when $a_z \ll q_z \ll 1$ the ion trajectory is dominated by the low-frequency secular motion $\omega_{r,z}$ and only weakly modulated by the micromotion at the RF frequency Ω ($\omega_{r,z} \ll \Omega$). Under these conditions, the ion secular frequency is approximately given as

$$\omega_i \sim \beta_i(\Omega/2),$$

with

$$\beta_i^2 = a_i + \frac{q_i^2}{2}. \tag{4}$$

In this approximation the ion oscillates in the potential well whose depth is given as [16]

$$D_{r,z} = \frac{m\Omega^2}{8e}(\beta_r^2 r_0^2 + \beta_z^2 z_0^2). \tag{5}$$

2. Experimental

Confinement of Eu ions in a RF quadrupole trap has been achieved and described in detail in ref. [17]. The radius of the ring electrode r_0 is 20 mm and the two end caps are $2z_0 = 28.28$ mm apart. The ion trap is mounted in an ultrahigh vacuum chamber bakeable up to 250°C. The base vacuum of 6×10^{-9} mbar was achieved by a combination of turbo-molecular pump and sputter ion pump. Eu ions were created in the trap by surface ionization of Eu metal placed on platinum filament, which is resistively heated. Cooling of the ions was achieved by introducing buffer gas into the ultrahigh vacuum chamber through a needle valve to the desired pressure. The typical operating voltages were, AC voltage $V_{\rm AC} = 446$ V, DC voltage at $U_{\rm DC} = 14$ V, driving frequency $\Omega/2\pi = 500$ kHz, resulting in $a_z = -0.01216$ and $q_z = 0.2829$. This provides the axial ($D_{\rm effz}$) and radial ($D_{\rm effr}$) potential well depth of 10.98 eV and 12.67 eV respectively.

The trapped ions are detected electronically [17] using a high impedance (2 MΩ) tank circuit (quality factor ∼80) connected across the end caps of the trap. The mid-point of the tank circuit is grounded to minimize the interference due to the

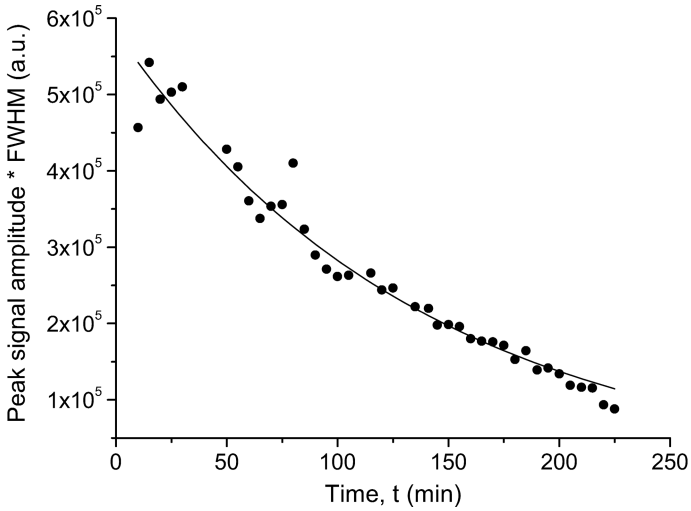

Figure 1. Decay of the trapped Eu^+ ion number with time, cooled by He at 5×10^{-6} mbar. The circles (•) are experimental points and the continuous curve is the least square fit to the exponential function.

high voltage source V_{AC}. The tank circuit is tuned and weakly coupled to a RF source fixed at frequency $\omega_0/2\pi = 58.5$ kHz, close to oscillation frequency ω_z of the ions in the z direction (secular frequency). The secular frequency ω_z of the trapped ions is brought into resonance with the detection frequency ω_0 of the tank circuit by sweeping the DC voltage (U_{DC}). At resonance, the trapped ions absorb energy from the RF source resulting in a drop in voltage across the tank circuit. This voltage is further amplified and demodulated by a tuned amplifier followed by an amplitude demodulator.

3. Results and discussion

3.1 *Storage time*

Optimizing the operating parameters, the best storage time of the Eu ions at a base vacuum of 6×10^{-9} mbar is found to be just 20 s. The trapped ions have kinetic energies of a few electron volts compared to the typical trap depths of tens of eV, leading to a high rate of ion loss. In addition hot ions will be more easily lost through collisions with background gases than cold ones. Thus cooling of the trapped ions is extremely important to increase the storage time. The decay of the total number of trapped ions $N(t)$ with time follows the expression $N(t) = N_0 \exp(-t/\tau)$, N_0 being the initial number of ions stored and τ is the storage time [8]. The trapped ion absorption signal was captured at fixed intervals of time and plotted against the product of peak signal amplitude and FWHM and is shown in figure 1. The storage time was obtained by fitting the experimental data to the exponential function.

Paul trap

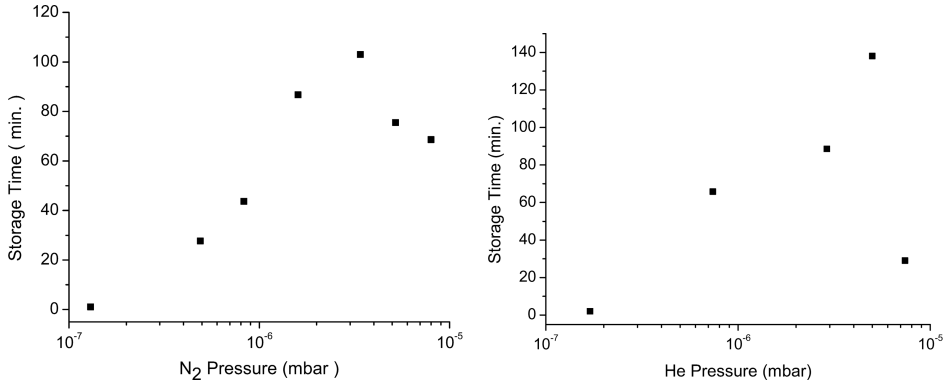

Figure 2. Plot of storage time versus (**a**) nitrogen pressure and (**b**) helium pressure.

The storage time for different buffer gas pressures was measured. Both N_2 and He were introduced separately into the ion trap chamber assembly through a needle valve. Figures 2a and 2b show the storage time obtained with N_2 and He buffer gas at different pressures. Using N_2 as buffer gas the best storage time of 103 min is obtained at 3.4×10^{-6} mbar pressure. At higher buffer gas pressures the storage time decreases due to loss of ions by diffusion [18].

With He as buffer gas the best storage time of 138 min was obtained at 5×10^{-6} mbar. A better storage time is obtained with He, as it is lighter than N_2 [9].

3.2 *Estimation of ion number*

Wineland and Dehmelt [19] have modeled the trapped particles as being bound between the parallel plate capacitor by a massless spring. When the trapped ions are probed by an external RF field and ion–ion, ion background particle collisions and trap imperfections are included in the damping term, the center of mass of the ion cloud, exhibits forced damped harmonic oscillations in the z direction. Then eq. (3) can be rewritten as

$$\frac{\mathrm{d}^2 Z}{\mathrm{d}t^2} + \gamma_2 \frac{\mathrm{d}Z}{\mathrm{d}t} + \omega_z^2 Z = \Gamma \frac{ev_0}{2mz_0}, \tag{6}$$

where γ_2 is the damping constant, Γ is a correction factor for non-parallel electrode and is equal to 0.86, m and e are the mass and charge of the trapped particle respectively, v_0 is the probing voltage appearing across the end caps.

The mean current induced by the forced damped motion of the trapped ions in the z direction is $\dot{q} = \Gamma(Ne/2z_0)\dot{Z}, q$ is the charge of the ion cloud in the trap. Substituting $\dot{q}$ in eq. (6) it is seen that the trapped ion system is equivalent to a series LCR circuit

$$L_i \ddot{q} + R_i \dot{q} + \frac{1}{C_i} q = v_0 \tag{7}$$

in which the inductance, resistance and capacitance have the values given by

$$L_i = \left(\frac{m}{N}\right)\ \left(\frac{2z_0}{\Gamma e}\right)^2; \quad R_i = \gamma_2 \left(\frac{m}{N}\right)\ \left(\frac{2z_0}{\Gamma e}\right)^2; \quad \frac{1}{C_i} = \omega_z^2 \left(\frac{m}{N}\right)\ \left(\frac{2z_0}{\Gamma e}\right)^2. \quad (8)$$

The electrical equivalent representation of ions confined in a Paul trap and external circuitry used in our set-up is shown in figure 3, where $Z = R_i + i\omega_0 L_i + (1/i\omega_0 C_i)$; and L, C and R are the inductance, capacitance and resistance respectively of the detection circuit. The voltage v_0 developed across the tank circuit is given as

$$v_0 = \omega_0 R C_E v_i - R\dot{q}. \quad (9)$$

Substituting v_0 in eq. (7)

$$L_i\ddot{q} + (R_i + R)\dot{q} + \frac{1}{C_i}q = \omega_0 R C_E v_i, \quad (10)$$

where $v_i = V_i \cos\omega_0 t$ is the voltage delivered by the RF source.

The impedance Z is changed by varying $U_{\rm DC}$ applied to the trap electrode, which in turn changes the ion secular frequency $\omega_z = 1/\sqrt{L_i C_i}$. The resonance condition is achieved when the external excitation frequency ω_0 matches with the ion secular frequency ω_z, i.e. the impedance offered by the ions is minimum. The relative ion response signal $Y = 1 - V_0/V_{00}$, where $V_{00} = \omega_0 R C_E V_i$ is the value of V_0 at the resonance frequency of tank circuit in the absence of ions [10]. At resonance the relative ion response signal is given as

$$Y = 1 - \left[\frac{\text{Re } Z^2 + \text{Im } Z^2}{(R + \text{Re } Z)^2 + \text{Im } Z^2}\right]^{1/2}, \quad (11)$$

where Re $Z = R_i$ and Im $Z = \omega_0 L_i - (1/\omega_0 C_i)$. .

A least square fit of the experimental RF absorption signal to the relative ion response signal yields the total number of ions trapped and the damping constant. Figure 4 shows a typical fit to the experimental absorption signal. Here $U_{\rm DC}$ is

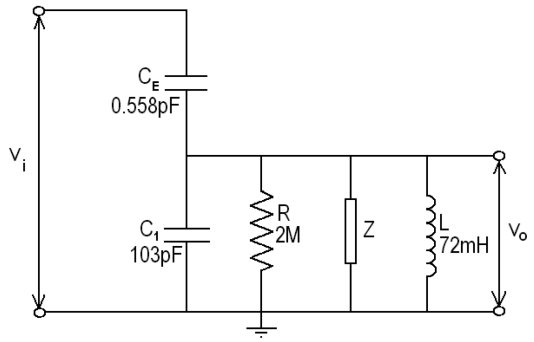

Figure 3. Electrical equivalent representation of trapped Eu^+ ions and the external detection circuitry.

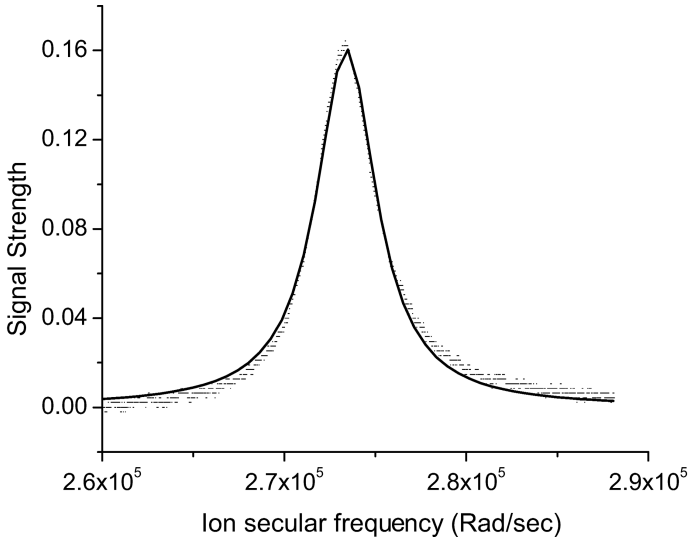

Figure 4. Least square fit (—) of the ions response signal to the experimental RF absorption signal (‖) of RF source at 29 mv.

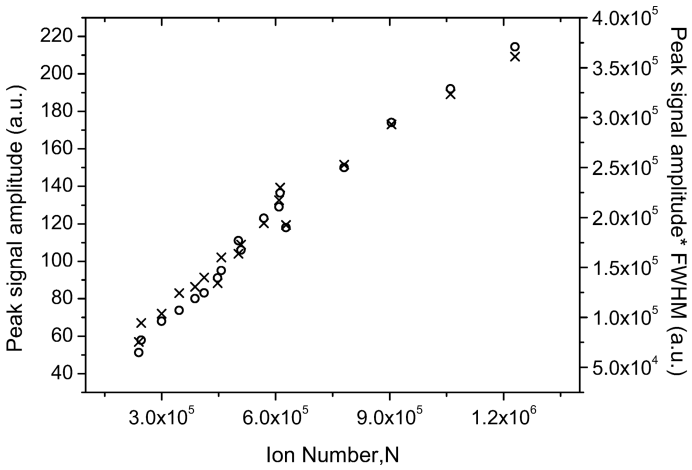

Figure 5. Plot of peak signal amplitude (○) and product of peak signal amplitude and FWHM (×) vs. ion number deduced from the fit.

swept from 10.6 V to 17 V in 250 ms and the He buffer gas pressure is maintained at 5×10^{-6} mbar. From the fit the total number of ions trapped is estimated to be $N = 3.69 \times 10^6$ and the damping constant $\gamma_2 = 3517$ rad/s. Figure 5 shows the relation between the estimated ion number and peak signal amplitude as well as the product of peak signal amplitude and FWHM. In the range of the number of ions trapped it shows that both the peak signal amplitude and the product of the peak signal amplitude and the FWHM is proportional to N.

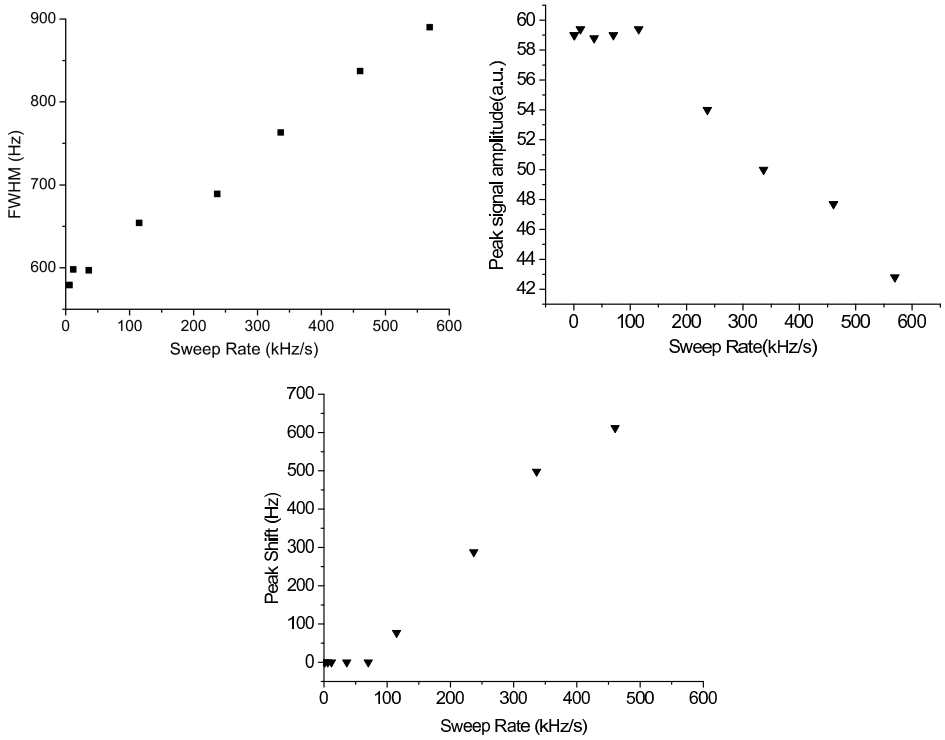

Figure 6. Experimentally measured (**a**) FWHM, (**b**) peak amplitude of signal and (**c**) shift in peak versus sweep rate.

3.3 *Effects of sweep rate*

The ion oscillation frequency was swept at different rates and its effect on the electronically detected trapped ion signal was measured experimentally. This set of experiment was carried out on the trapped Eu ion cloud at He buffer gas pressure of 5×10^{-6} mbar. The data were collected within a time period during which the ion number was more or less a constant. The peak signal amplitude, FWHM and the frequency shift of the peak were measured at different sweep rates ranging from 6 kHz/s to 570 kHz/s (the time constant of the detection circuit is 2 ms). Figure 6 shows the effect of sweep rate on the detected signal: (a) the FWHM increases as sweep rate increases, (b) the peak amplitude of the signal decreases as sweep rate increases, (c) the peak of the signal shifts towards higher frequency with increasing sweep rate.

Assuming that (i) the secular frequency of ions ω_z is swept linearly and brought into resonance of the tank circuit (frequency, ω_0) i.e. $\omega_z + at = \omega_0$ where a is the sweep rate, (ii) the charge $q(t)$ and RF source voltage v_i are expressed as $q(t) = Q(t)\exp(j\omega_0 t)$ and $v_i = V_i \exp(j\omega_0 t)$ and (iii) $Q(t)$ changes slowly, eq. (10) can be approximated as [20]

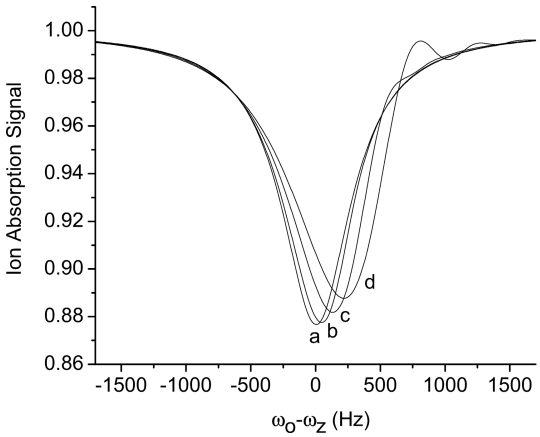

Figure 7. Plot of the rf absorption signal vs. detuning ($\omega_0 - \omega_z$ (Hz)) at different sweep rates (**a**) 6, (**b**) 70, (**c**) 237 and (**d**) 460 kHz/s.

$$\frac{\mathrm{d}Q}{\mathrm{d}t} + \left(\frac{1}{2T_0} + jat\right) Q(t) = \frac{RC_E}{2L_i} V_i, \tag{12}$$

where $1/T_0 = (R_i + R)/L_i$.

This is a complex differential equation of Leibnitz linear form in time. The solution of the above equation has the following form: $Q(t) = (u(t) + jv(t))V_i$ [21]. Substituting the expression of induced ion current $\dot{q} = j\omega_0(u + jv)V_i \mathrm{e}^{j\omega_0 t}$ into eq. (9), we obtain the following amplitude of the RF voltage:

$$|v_0| = V_i \omega_0 R \sqrt{(C_E - u)^2 + v^2}. \tag{13}$$

The values of u and v are numerically computed using the following equations:

$$\begin{aligned} u(x) = \alpha \mathrm{e}^{-Ax} &\left[\cos\left(\frac{x^2}{2}\right) \int_{-\infty}^{x} \mathrm{e}^{Ax} \cos\left(\frac{x'^2}{2}\right) \mathrm{d}x' \right. \\ &\left. + \sin\left(\frac{x^2}{2}\right) \int_{-\infty}^{x} \mathrm{e}^{Ax'} \sin\left(\frac{x'^2}{2}\right) \mathrm{d}x' \right], \\ v(x) = \alpha \mathrm{e}^{-Ax} &\left[-\sin\left(\frac{x^2}{2}\right) \int_{-\infty}^{x} \mathrm{e}^{Ax'} \cos\left(\frac{x'^2}{2}\right) \mathrm{d}x' \right. \\ &\left. + \cos\left(\frac{x^2}{2}\right) \int_{-\infty}^{x} \mathrm{e}^{Ax} \sin\left(\frac{x'^2}{2}\right) \mathrm{d}x' \right], \end{aligned} \tag{14}$$

where

$$A = \frac{1}{2T_0\sqrt{a}}; \quad x = \sqrt{at}; \quad \alpha = \frac{RC_E}{2L_i\sqrt{a}}.$$

The simulated signal line shape is computed typically for four different sweep rates matching with that employed in the experiment and is shown in figure 7. The simulations show a decrease in peak signal amplitude, increase in FWHM and

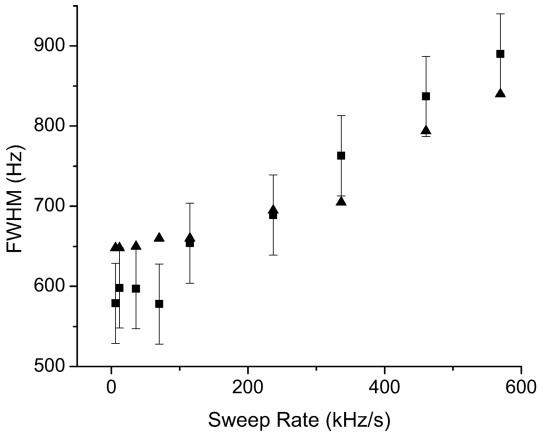

Figure 8. Plot of experimental (■) and simulated (▼) FWHM (Hz) vs. sweep rate (kHz/s).

the peak shifts towards higher frequency side with increasing sweep rate. The simulations are in qualitative agreement with our experimental findings. Figure 8 shows the effect of sweep rate on the FWHM observed experimentally and estimated by simulations. In our simulations the damping constant γ_2 is taken to be 3517 rad/s and the total number of trapped ions $N = 3.69 \times 10^6$ as obtained from fit (see figure 4). It is seen that our simulation results matches well with the experimental data within the experimental error ($\sim \pm$ 50 Hz).

4. Conclusion

The non-destructive electronic detection technique, best suited for detection of ion clouds, has been employed and the ion number and storage time is estimated at very low excitation RF amplitude and low sweep rate.

The storage time of trapped ions of 20 s in vacuum was improved by employing buffer gas cooling to 138 min with optimum He pressure at 5×10^{-6} mbar. The number of ions trapped was estimated from the least square fit of the experimental RF absorption signal to the theoretical ion response profile. It is found that the product of the FWHM and the peak signal amplitude as well as just the peak signal amplitude are both linearly dependent on the total number of trapped ions in the range of the number of ions trapped.

Line profile analysis of the experimental RF absorption signal was carried out at different sweep rates. Simulations are carried out at the same sweep rates and compared with the experimental data and the agreement is good.

References

[1] R E March and J F Todd, *Practical aspects of ion trap mass spectrometery* (CRC Press, USA, 1995) vol. III

[2] G Werth, *Phys. Scr.* **T22**, 191 (1988)
[3] D J Berkeland, J D Miller, F C Cruz, B C Cruz, B C Young, J C Bergquist, W M Itano and D J Wineland, *Proc. 2nd Int. Symp. on Modern Problems of Laser Physics* edited by S N Bagayev and V I Denisov, *Laser Physics* **8**, 673 (1998)
[4] G Werth, *Hyperfine Interactions* **99**, 3 (1996)
[5] F G Major, V N Gheorghe and G Werth, *Charged particle traps* (Springer Verlag Germany, 2004)
[6] W Paul, O Osberghaus and E Fischer, *Forschungsber. Wirtsch. Verkehrsminist. Nordrhein-Westfalen* **415**, 5 (1958)
[7] W Neuhauser, M Hohenstatt, P E Toschek and H Dehmelt, *Phys. Rev.* **A22**, 1137 (1980)
[8] D A Church and H G Dehmelt, *J. Appl. Phys.* **40**, 3421 (1969)
[9] F G Major and H G Dehmelt, *Phys. Rev.* **170**, 91 (1968)
[10] M N Gaboriaud, M Desaintfuscien and F G Major, *Int. J. Mass Spectrom. Ion Phys.* **41**, 109 (1981)
[11] D E Goeringer, W B Whitten, J M Ramasey, S A McLuckey and G L Glish, *Annal. Chem.* **64**, 1434 (1992)
[12] A Makarov, *Anal. Chem.* **68**, 4257 (1996)
[13] N W McLachlan, *Theory and application of Mathieu functions* (Oxford University Press, London, 1951)
[14] M Abromowitz and I A Stegun, *Handbook of mathematical functions* (Dover Publications Inc., New York, 1970)
[15] R F Wuerker, H Shelton and R V Langmuir, *J. Appl. Phys.* **30**, 342 (1959)
[16] H Dehmelt, *Adv. At. Mol. Phys.* **3**, 53 (1967)
[17] P M Rao, S Bhattacharayya, S G Nakhate and G Joshi, *Curr. Sci.* **85**, 72 (2003)
[18] D A Church, *Phys. Rep.* **228**, 253 (1993)
[19] D J Wineland and H Dehmelt, *J. Appl. Phys.* **46**, 919 (1975)
[20] Y Yoda and K Sugiyama, *Jpn. J. Appl. Phys.* **24**, L1738 (1987)
[21] B A Jacobson and R K Wangsness, *Phys. Rev.* **73**, 942 (1948)